Chapter 2
The Marine CO_2 System and Its Peculiarities in the Baltic Sea

2.1 Atmospheric CO_2 Over the Baltic Sea

Due to its solubility and chemistry in aqueous solutions, CO_2 is distributed in a characteristic manner between the atmosphere and ocean waters. CO_2 inventories in these two compartments are coupled by gas exchange and are therefore mutually dependent. This is highly important for the atmospheric CO_2 budget, which has been strongly perturbed by anthropogenic CO_2 emissions. From the CO_2 released into the atmosphere mainly by the combustion of fossil fuel during the past $\sim$200 years, $\sim$30% has been taken up by the world's oceans (Le Quéré et al. 2016). This has considerably mitigated the increase in atmospheric CO_2 concentrations, which are currently at $\sim$400 ppm (https://www.esrl.noaa.gov/gmd/ccgg/trends/). Although in the south the Baltic Sea borders heavily urbanized and industrialized areas, the atmospheric CO_2 concentration differs only slightly from those determined at background stations in the northern hemisphere. An example is given in Fig. 2.1, which shows the CO_2 concentrations in the atmosphere over the Baltic Sea in 2005 (Schneider et al. 2014). On average, they deviate only by 3 ppm from those at the remote station in Barrow, Alaska. Likewise, the seasonal peak-to-peak amplitudes of the atmospheric CO_2 concentrations ($\sim$17 ppm) caused by the uptake and release of CO_2 by the terrestrial biosphere do not show significant regional differences. The low impact of regional CO_2 sources on the atmospheric CO_2 level is due to rapid atmospheric mixing and the relatively long residence time of CO_2 in the atmosphere. The latter implies high mean concentrations and less influence of local or regional sources.

B. Schneider and J.D. Müller, *Biogeochemical Transformations in the Baltic Sea*,
Springer Oceanography, DOI 10.1007/978-3-319-61699-5_2

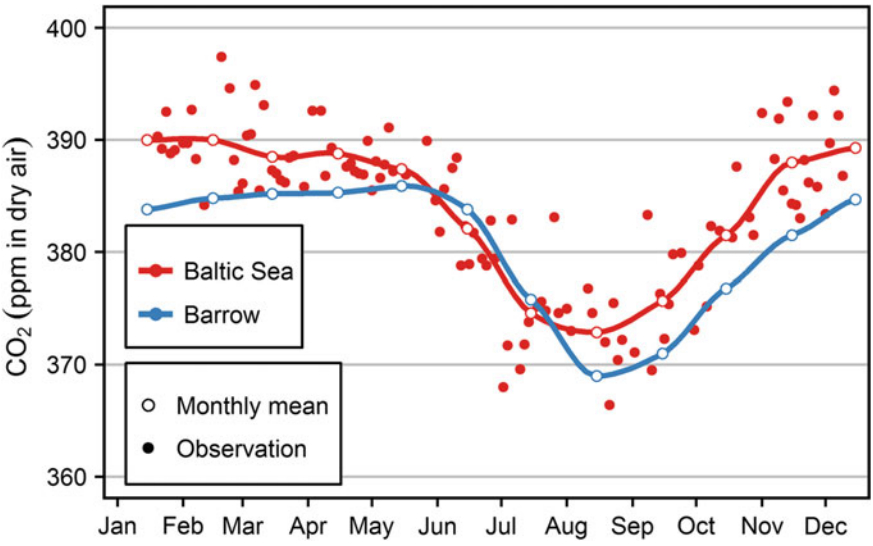

Fig. 2.1 Atmospheric CO_2 concentrations in the Baltic Sea area (58°N, 20°E, *red*) and at the northern hemispheric background station, Barrow, Alaska (71°N, 156°W, *blue*) in 2005. Only small differences with respect to the mean values and the seasonal amplitude exist

2.2 Aqueous Equilibrium Chemistry of CO_2

Once CO_2 is physically dissolved in water, it undergoes hydration and forms carbonic acid (Eq. 2.1):

$$CO_2 + H_2O \Leftrightarrow H_2CO_3 \tag{2.1}$$

This reaction is at equilibrium when the CO_2 and H_2CO_3 concentrations satisfy Eq. 2.2:

$$\frac{[H_2CO_3]}{[CO_2]} = K_{hyd} \tag{2.2}$$

The equilibrium between dissolved CO_2 and H_2CO_3 is thus characterized by the hydration constant $K_{hyd.}$

This is the first in a series of equilibrium reactions that control the abundance of CO_2 species in seawater. The chemical equilibria of this and all other chemical reactions concerning the marine CO_2 system are expressed in terms of concentrations rather than activities (Box 2.1). This convention applies to all CO_2 equilibria described in the following sections and all concentrations regarding CO_2 system variables are expressed as moles per mass seawater.

Box 2.1: Activities and concentrations
The activity (a) of a dissolved species is related to its concentration (c) by the activity coefficient γ:

$$a = \gamma \cdot c \tag{B2.1}$$

which accounts for the change in the chemical potential of a chemical species due to its interactions with any other solute. Classical thermodynamic equilibrium constants are based on activities and depend on temperature and pressure. However, equilibrium constants describing the marine CO_2 system are generally expressed in terms of concentration, which is more easily accessible by chemical analysis. Hence, a concentration-based equilibrium constant implicitly includes the corresponding activity coefficient. This implies that the equilibrium constants describing the marine CO_2 system depend also on salinity, which represents the major solute in seawater and is thus controlling the activity coefficient. This convention, together with the use of the concentration in units of moles per mass seawater, applies to all CO_2 equilibria described in the following sections.

The CO_2 hydration constant K_{hyd} (S = 35, T = 25 °C) is 1.2×10^{-3} (Soli and Byrne 2002) and indicates that only about one per mille of dissolved CO_2 exist as undissociated carbonic acid. Since H_2CO_3 molecules do not have a specific function in biogeochemical transformations, they are not explicitly included in the characterization of the marine CO_2 system; instead, the sum of the CO_2 and H_2CO_3 concentrations is used, expressed as the variable CO_2^* (synonymous to $H_2CO_3^*$) (Eq. 2.3):

$$[CO_2^*] = [CO_2] + [H_2CO_3] \tag{2.3}$$

which thus describes the solubility of CO_2 in seawater. The equilibrium between CO_2 in the gas phase and CO_2* dissolved in seawater is characterized by the solubility constant, K_0 (Eq. 2.4), which depends on temperature, pressure, and salinity (Weiss 1974). The pressure dependency of K_0 refers to the total pressure that acts upon the considered water body and is a function of water depth (Eq. 2.4).

$$[CO_2^*] = K_0 \cdot fCO_2 \tag{2.4}$$

where fCO_2 is the fugacity, expressed in pressure units. It determines the chemical potential of CO_2 in the gas phase and is thus analogous to the activity of dissolved species. It deviates slightly from the CO_2 partial pressure, pCO_2, due to the non-ideal behavior of CO_2. However, because the pCO_2 is directly accessible by measurements, our considerations of the CO_2 system will consistently use pCO_2, which for computations concerning the marine CO_2 system is then converted by the currently available software to fCO_2 (e.g., Pierrot et al. 2006; Lavigne et al. 2011).

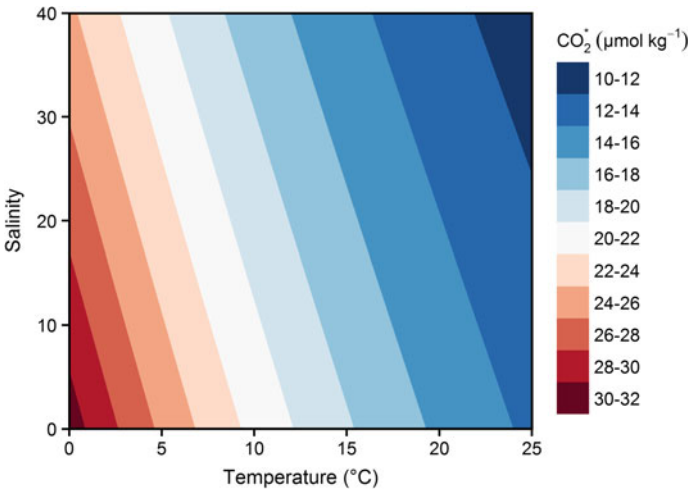

Fig. 2.2 CO_2^* concentrations of seawater at equilibrium with an atmospheric pCO_2 of 400 µatm. The pattern reflects the salinity and temperature dependence of the CO_2 solubility constant K_0

To illustrate variations in the solubility constant, K_0, the concentrations of CO_2^* at equilibrium with an atmospheric pCO_2 = 400 µatm are shown as a function of temperature and salinity in Fig. 2.2. The solubility constant and thus CO_2^* concentrations decrease with increasing temperature and salinity. The concentrations span a wide range and are as low as 12 µmol kg^{-1} at an oceanic salinity of 35 and a temperature of 25 °C but may be as high as >30 µmol kg^{-1} in river water with a salinity of ~0 and a temperature of 0 °C.

Carbonic acid produced by the hydration of CO_2 dissociates in a first step according to Eq. 2.5:

$$H_2CO_3 \Leftrightarrow HCO_3^- + H^+ \tag{2.5}$$

During the dissociation of an acid, hydrogen ions (protons) are transferred to a water molecule or to a cluster of several water molecules. Although free protons do not exist, it is common practice to denote combinations of protons and water molecules (e.g., H_3O^+) by H^+. The equilibrium condition for the first dissociation step of H_2CO_3 is given by Eq. 2.6:

$$\frac{[H^+] \cdot [HCO_3^-]}{[H_2CO_3]} = K_a \tag{2.6}$$

The dissociation constant, K_a, at 25 °C and 0 salinity is 2.5 × 10^{-4} mol kg^{-1}. This means that carbonic acid is a relatively strong acid, with a pK_a similar to that of formic acid. However, the acidity (pH) of carbonic acid dissolved in pure water is constrained by the equilibrium with dissolved CO_2 (Eqs. 2.1 and 2.2), which in turn is limited by the equilibrium with gas-phase CO_2. Only a small fraction of the

dissolved CO_2 is transferred to H_2CO_3 and can thus act as an acid. It is therefore convenient to combine the hydration and the first dissociation equilibria and to describe the acidity of carbonic acid as a function of the dissolved CO_2 concentration, as shown in Eq. 2.7:

$$CO_2 + H_2O \Leftrightarrow [HCO_3^-] + [H^+] \tag{2.7}$$

Taking into account the CO_2 hydration equilibrium (Eq. 2.2), the first dissociation equilibrium of H_2CO_3 (Eq. 2.6), and the definition of CO_2^* (Eq. 2.3) yields the equilibrium condition for the reaction shown in Eq. 2.7 (see Box 2.2 for the derivation):

$$\frac{[H^+] \cdot [HCO_3^-]}{[CO_2^*]} = K_1 \tag{2.8}$$

with:

$$K_1 = K_a \cdot \frac{K_{hyd}}{1 + K_{hyd}} \tag{2.9}$$

where K_1 is the first dissociation constant of the marine CO_2 system (Eqs. 2.8 and 2.9), which includes both the dissociation constant of carbonic acid and the hydration constant (Eq. 2.9). Since $K_{hyd} \ll 1$, K_1 approximately equals the product of $K_a \times K_{hyd}$. During the last 20–30 years, intensive efforts have been directed at

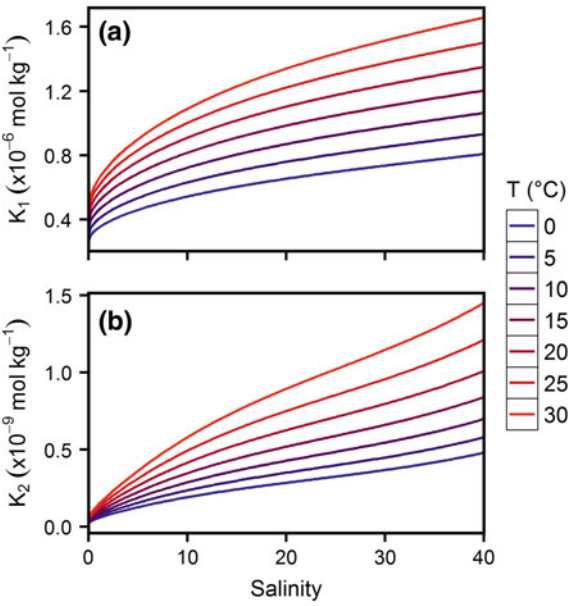

Fig. 2.3 Dissociation constants of the marine CO_2 system: **a** The first dissociation constants K_1 refers to CO_2^* (CO_2 + H_2CO_3) and **b** the second dissociation constant, K_2, to HCO_3^-

establishing equations that describe K_1 as a function of temperature, salinity, and pressure (an overview is given in Pierrot et al. 2006), with most focusing on the salinity range encountered in ocean waters. The only equation that also refers to brackish water and is consistent with the well-established K_1 for freshwater was published by Millero et al. (2006) and refined in Millero et al. (2010). The K_1 values obtained from this equation are plotted in Fig. 2.3a as a function of salinity (0–40) for temperatures between 0 and 20 °C. Within this range of conditions, the dissociation constant K_1 varies by almost one order of magnitude and, expressed as the negative decadal logarithm, is in the range of $6.6 > p\,K_1 > 5.8$. Dissociation is enhanced at high temperatures and increases with increasing salinity. The salinity dependency is especially pronounced at salinities below 10, which are characteristic for the Baltic Proper and its adjacent gulfs.

During the second dissociation step, hydrogen carbonate ions transfer another proton to water molecules (Eq. 2.10):

$$HCO_3^- \Leftrightarrow CO_3^{2-} + H^+ \tag{2.10}$$

The corresponding equilibrium equation is shown in Eq. 2.11:

$$\frac{[CO_3^{2-}] \cdot [H^+]}{[HCO_3^-]} = K_2 \tag{2.11}$$

Qualitatively, the temperature and salinity dependencies of K_2 (Millero 2010) are similar to those of K_1. However, the range of K_2 is clearly larger, covering more than one order of magnitude ($10.6 > pK_2 > 8.8$) with respect to the limiting values used in Fig. 2.3b (**S** = 0–40, **T** = 0–30 °C).

Finally, the solubility of solid calcium carbonate has an impact on the marine CO_2 system. The formation of calcium carbonate shells by various marine organisms is a widespread phenomenon in ocean waters. However, in the Baltic Sea the abundance of calcifying plankton such as coccolithophores is significant only in the transition area between the Baltic Sea and the North Sea (Tyrrell et al. 2008). Biogenic calcium carbonate occurs in two different crystalline phases, either as calcite or aragonite. The solubility is characterized by the solubility product, K_{sp} (Eq. 2.12):

$$[Ca^{2+}] \cdot [CO_3^{2-}] = K_{sp} \tag{2.12}$$

Box 2.2: Derivation of the first dissociation constant of the marine CO_2 system, K_1

The equilibrium condition for the dissociation of the first hydrogen ion of carbonic acid constitutes the basis for the first dissociation constant, K_1, of the marine CO_2 system:

$$\frac{[H^+] \cdot [HCO_3^-]}{[H_2CO_3]} = K_a \tag{B2.1}$$

It is related to the hydration equilibrium:

$$\frac{[H_2CO_3]}{[CO_2]} = K_{hyd} \tag{B2.2}$$

Taking into account the definition of CO_2^*:

$$[CO_2^*] = [CO_2] + [H_2CO_3] \tag{B2.3}$$

and combining with B2.2, CO_2^* can be expressed by:

$$[CO_2^*] = \frac{[H_2CO_3]}{K_{hyd}} + [H_2CO_3] \tag{B2.4}$$

or:

$$[H_2CO_3] = [CO_2^*] \cdot \frac{K_{hyd}}{1 + K_{hyd}} \tag{B2.5}$$

Introducing B2.5 into B2.1, yields

$$\frac{[H^+] \cdot [HCO_3^-]}{[CO_2^*]} = K_a \cdot \frac{K_{hyd}}{1 + K_{hyd}} \tag{B2.6}$$

Hence, the conversion of CO_2^* to H^+ and HCO_3^- is characterized by an equilibrium constant, K_1, that is a composite of K_a and K_{hyd}:

$$\frac{[H^+] \cdot [HCO_3^-]}{[CO_2^*]} = K_1 \tag{B2.7}$$

$$K_1 = K_a \cdot \frac{K_{hyd}}{1 + K_{hyd}} \tag{B2.8}$$

In the case of calcite, K_{sp} is almost independent of temperature but increases strongly with increasing salinity, as shown in Fig. 2.4a. The change of K_{sp} with

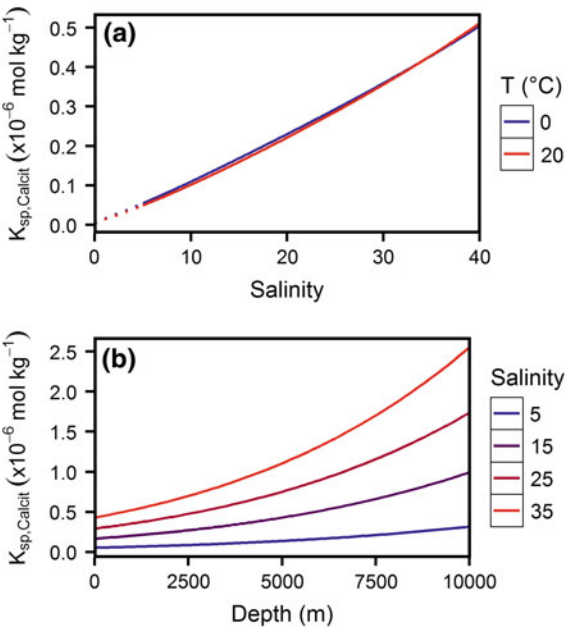

Fig. 2.4 The solubility product of calcite **a** as a function of salinity at different temperatures in surface water and **b** as a function of water depth at different salinities and T = 5 °C

pressure, expressed in terms of water depth in Fig. 2.4b, is even more pronounced. The calcite solubility at a depth of 10,000 m (T = 5 °C; S = 35) is 750-fold higher than in river water (T = 20 °C; S = 0). The solubility of aragonite is larger and in dependence on the physical conditions, the K_{sp} of aragonite exceeds that of calcite by a factor of 1.5–1.6.

Chemical equilibria between ionic CO_2 species are established almost spontaneously and also the hydration of CO_2, although slower, still occurs on a time scale of only seconds. By contrast, the dissolution of calcite or aragonite is a significantly slower process (Milliman 1975), resulting in the delayed establishment of the respective solubility equilibria. The degree of saturation (Ω) is defined as the ratio between the actual product of the concentration of Ca^{2+} and CO_3^{2-} ions and the solubility product, as shown in Eq. 2.13:

$$\Omega = \frac{[Ca^{2+}] \cdot [CO_3^{2-}]}{K_{sp}} \tag{2.13}$$

Although ocean surface waters are generally oversaturated with calcite ($\Omega > 4$), chemical precipitation of $CaCO_3$ does not occur because it is kinetically inhibited by magnesium ions (Berner 1975). Yet, calcifying organisms possess biochemical "tools" which enable them to overcome this inhibition and are even able to build $CaCO_3$ shells in waters that are undersaturated with $CaCO_3$. Considerable $CaCO_3$ oversaturation also characterizes river water and plays an important role in the input of alkalinity into the Baltic Sea (see Sect. 2.3.3).

2.3 Measurable Variables of the Marine CO_2 System

2.3.1 CO_2 Equilibrium Fugacity and Partial Pressure

Concentrations of CO_2^*, shown as a function of temperature and salinity in Fig. 2.2, refer to the equilibrium between the surface water and the atmospheric CO_2 fugacity (fCO_2). However, this equilibrium generally does not exist in nature because the gas exchange that is a prerequisite for its establishment always lags behind continuous changes in the surface-water equilibrium fCO_2 caused by changes in either temperature or the CO_2* concentration. In case of a temperature increase or decrease, both the solubility constant and, due to the dissociation equilibria, CO_2*, change. Hence, the equilibrium fCO_2 increases or decreases according to Eq. 2.14:

$$fCO_2 = \frac{[CO_2^*]}{K_0} \tag{2.14}$$

Similarly, any change in [CO_2*] that may occur as a result of biomass production or mineralization will affect the equilibrium fCO_2. The equilibrium fCO_2 is a fundamental property of a water mass and independent of the existence of a gas phase in contact with this water mass. For reasons of practicability, the equilibrium fCO_2 of seawater is commonly denoted simply as "fCO_2", in contrast to the atmospheric "fCO_2^{atm}". In the characterization of the marine CO_2 system, fCO_2 is an important variable because it is directly related to the concentration of CO_2* (Eq. 2.4), which yields HCO_3^- and CO_3^{2-} by the dissociation of carbonic acid. However, pCO_2 that at atmospheric pressure and composition deviates only very slightly from the fCO_2 is typically used to describe the status of the marine CO_2 system. Nonetheless, for further calculations concerning the CO_2 system, the use of software that converts pCO_2 to fCO_2 is recommended.

2.3.2 Total CO_2 and pH

C_T is the sum of the chemical species generated by the dissolution and dissociation of CO_2 in water and it is sometimes referred to as "dissolved inorganic carbon" (DIC) (Eq. 2.15):

$$C_T = [CO_2^*] + [HCO_3^-] + [CO_3^{2-}] \tag{2.15}$$

Typical C_T concentrations in pure water and surface seawater from the central Baltic and the ocean are shown in Fig. 2.5b. The bars in the figure represent the C_T at 10 °C and at equilibrium with an atmospheric pCO_2 of 400 µatm. The C_T of pure water ($\sim$25 µmol kg^{-1}) is 70- to 90-fold lower than that of seawater and $\sim$90% is contributed by CO_2*; hence, it mainly consists of dissolved molecular CO_2.

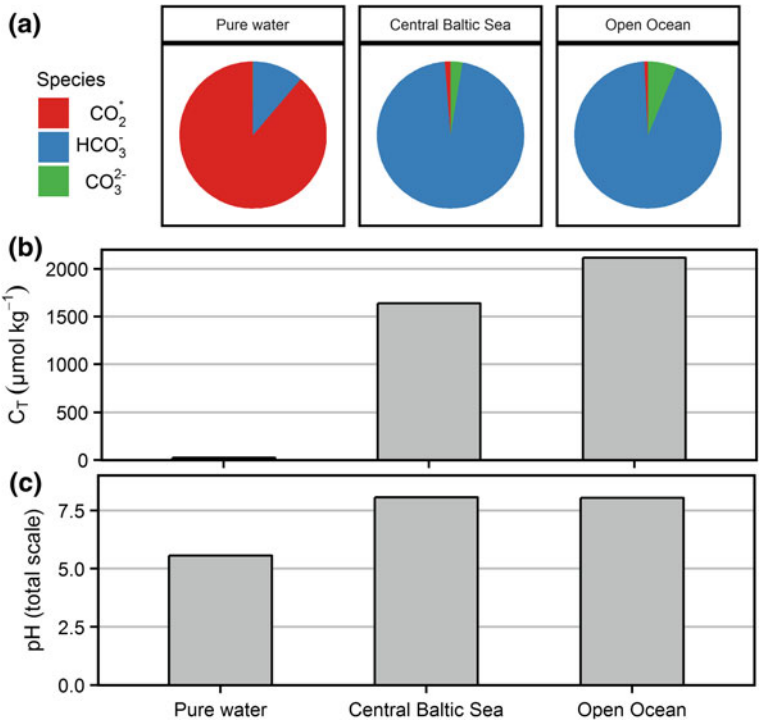

Fig. 2.5 Comparison between pure water, Baltic Sea water and ocean water concerning: **a** relative distribution of different CO_2 species, **b** the total amount of CO_2 (C_T), and **c** the pH (Computed for T = 10 °C, pCO_2 = 400 µatm; pure water: S = 0 and A_T = 0 µmol kg^{-1}, Baltic Sea: S = 7 and A_T = 1670 µmol kg^{-1}, ocean: S = 35 and A_T = 2300 µmol kg^{-1})

By contrast, in surface seawater, the CO_2* fraction accounts for only ~1% of C_T (red sections in Fig. 2.5a) and it is the C_T contribution of HCO_3^- (>90%; blue sections in Fig. 2.5a) that prevails. In pure water, the contribution of HCO_3^- is much lower (10%) and almost no (10^{-4}%) CO_3^{2-} ions are produced (green sections in Fig. 2.5a) during the dissolution of CO_2. Seawater is also low in CO_3^{2-}, but the contributions of the latter to C_T in the Baltic Sea and ocean water (3 and 6%, respectively) are significant and play an important biogeochemical role. The very large differences in the levels and composition of C_T between freshwater and seawater can be attributed to the alkalinity (A_T), which is another central variable in the marine CO_2 system (Sect. 2.3.3).

The concentrations of the different CO_2 species are coupled by the hydrogen ions generated during the stepwise dissociation of carbonic acid. The hydrogen ions control the two dissociation equilibria and, hence, the respective equations (Eqs. 2.8 and 2.11) include the hydrogen ion concentration and a reliable estimate of pH—the negative logarithm of the H^+ concentration—is an important piece of information to characterize the marine CO_2 system. However, the use of concentration units to describe dissociation equilibria conflicts with the traditional method

for the determination of pH in seawater, which is based on potentiometric measurements performed with glass electrodes and on calibrations with pH buffers dissolved in pure water (NBS buffer). While this has been the standard procedure for many decades and is still common practice in many fields of environmental research, it has several shortcomings with respect to pH determinations in seawater because the obtained pH refers to the so-called NBS scale and reflects neither the hydrogen ion activity (Box 2.1) nor the hydrogen ion concentration (Dickson 1984). To overcome this conceptual problem, pH buffers prepared in artificial seawater were introduced. This leads to pH scales in which the standard reference state for the hydrogen ion activity no longer refers to the thermodynamic properties in pure water but to a solution of hydrogen ions in artificial standard seawater of defined salinity (ionic media scale). Hence, any interactions between hydrogen ions and seawater ions are no longer accounted for by the activity coefficient but are characteristics of the solute-solvent interactions. This convention allows the activity coefficient of the hydrogen ions to be set to unity and leads to a pH scale based on concentration units.

Since sulfate is a major seawater component, it should be included in the composition of the artificial seawater used as the solvent for buffer solutions. However, this implies that the interaction of hydrogen ions with the solvent is not confined to the protonation of water molecules, e.g., by the formation of hydronium ions (H_3O^+), but also includes the formation of hydrogen sulfate (HSO_4^-). The sum of the two is called the "total hydrogen ion" concentration (Eq. 2.16):

$$[H_T^+] = [H_F^+] + [HSO_4^-] \tag{2.16}$$

where H_F^+ represents the protonated water molecules referred to as "free hydrogen ions." If the artificial seawater contains fluoride, the formation of HF must also be taken into account and yields the so called seawater pH scale: $[H_{SWS}^+] = [H_F^+] + [HSO_4^-] + [HF]$, which, however, has been largely replaced by the H_T^+ concentration scale.

Using the HSO_4^- dissociation constant, K_S, and assuming a constant sulfate concentration, $[SO_4^{2-}]$, that depends only on salinity, H_T^+ can be expressed as shown in Eq. 2.17:

$$[H_T^+] = [H_F^+] \cdot \left(1 + \frac{[SO_4^{2-}]}{K_S}\right) \tag{2.17}$$

In ocean water (S = 35), by definition $[H_{SWS}^+] > [H_T^+] > [H_F^+]$, which is reflected in a pH_T that is $\sim$0.09 units lower than pH_F, and pH_{SWS}, which in turn is about 0.01 units below the pH_T at 20 °C. These differences decrease with decreasing salinity. An exact thermodynamic determination of the differences between the NBS scale and the concentration scales at different salinities is not possible, but a difference of 0.13 pH units at a salinity of 35 is a reasonable estimate. In the following sections, we consistently refer to the pH on the total scale (pH_T) and use equilibrium constants that are based on it.

The pH_T of surface seawater is ~ 2 units higher than that of pure water at equilibrium with atmospheric CO_2 (Fig. 2.5c). Furthermore, the seawater CO_2 system is characterized by H^+ ion concentrations of $\sim 10^{-8}$ mol kg^{-1}, which is 3–5 orders of magnitude lower than the concentrations of the other dissociation products, HCO_3^- and CO_3^{2-}. Hence, the dissociation equilibria are very sensitive to $[H^+]$ perturbations by the direct input of an acid or by the addition/removal of CO_2 that results in carbonic acid generation. The re-equilibration of the CO_2 system consequently requires the removal of the bulk of the added H^+ ions, mainly by the protonation of CO_3^{2-} ions.

Measurements of C_T and pH may be used to calculate the concentrations of the different CO_2 species in seawater, provided that the dissociations constants K_1 and K_2 (Eqs. 2.8 and 2.11) as a function of temperature and salinity are known. Similarly, the pCO_2, which is related to CO_2^* by the solubility constant K_0, in combination with pH or C_T allows the full determination of the marine CO_2 system.

2.3.3 Alkalinity

Alkalinity is another central quantity for the characterization of the marine CO_2 system. It merits a separate section because: (i) it not only impacts the marine CO_2 system, but also refers explicitly to all acid-base constituents in seawater and (ii) it constitutes the link between biogeochemical processes on land and those in the sea. In the early stages of research on the marine CO_2 system, alkalinity was also termed the "acid binding capacity." This more illustrative term reflects the precise definition that considers alkalinity as the excess of proton acceptors over proton donors. In this context, proton acceptors are the anions of weak acids ($K_a < 10^{-4.5}$ mol kg^{-1}) whereas proton donors are strong acids ($K_a > 10^{-4.5}$ mol kg^{-1}) (Dickson 1981). For ocean surface waters, total alkalinity (A_T) is sufficiently represented by Eq. 2.18:

$$A_T = [HCO_3^-] + 2[CO_3^{2-}] + [B(OH)_4^-] + [OH^-] - [H_T^+] \tag{2.18}$$

where, in addition to HCO_3^- and CO_3^{2-} (carbonate alkalinity), borate and hydroxide ions are included as proton acceptors and the total hydrogen ion concentration, H_T^+, represents strong acids, such as protonated water molecules and HSO_4^- ions (Eq. 2.18). Alkalinity may be determined by different methods of titration using a strong acid. In the direct potentiometric titration with HCl, the excess of proton acceptors is compensated for by the amount of protons added during the titration and an analysis of the titration curve yields the equivalence point, indicated by an inflection point.

In the characterization of the CO_2 system using the measured A_T, non-CO_2 A_T contributions are expressed as a function of pH. In a simplified representation of A_T according to Eq. 2.18, this yields (Eq. 2.19):

$$A_T = [HCO_3^-] + 2[CO_3^{2-}] + B_T \cdot \frac{K_B}{[H_T^+] + K_B} + \frac{K_W}{[H_T^+]} - [H_T^+] \tag{2.19}$$

Since the boric acid dissociation constant, K_B, and the ion product of water, K_W, are thermodynamic constants that are known as functions of temperature and salinity, and since the total boric acid ($H_3BO_3 + B(OH)_4^-$) concentration, B_T, in seawater is a function of salinity, A_T is exclusively described by variables that characterize the marine CO_2 system (Eq. 2.19). Therefore, A_T together with any other variable (either pCO_2, pH, or C_T) and the carbonic acid (CO_2) dissociation constants provides a full characterization of the marine CO_2 system. In semi-enclosed marine systems such as the Baltic Sea and the Black Sea, where the development of anoxic conditions in deeper water layers is a common feature, the accumulation of phosphate and the formation of S^{2-} (at equilibrium with H_2S, HS^-) and ammonia also contribute significantly to the pool of proton acceptors and must be accounted for in Eq. 2.19. In this case, the acid-base components are independent of salinity and their total concentrations must be obtained from measurements. This also applies to any other additional alkalinity contributions, such as organic proton acceptors (Kulinski et al. 2014).

Another important aspect of the occurrence of alkalinity is the question for the processes that produce the excess of proton acceptors in seawater. Or in other words: what are the sources and sinks of alkalinity? The dissolution of gaseous CO_2 in pure water or in an acid/base-free seawater medium and the subsequent dissociation of carbonic acid cannot generate alkalinity because charge balance requires the production of equal amounts of proton acceptors and donors (Eq. 2.19):

$$\Delta[HCO_3^-] + 2\Delta[CO_3^{2-}] + \Delta[OH^-] = \Delta[H_T^+] \tag{2.20}$$

hence, $\Delta A_T = 0$. Instead, it is river water that transports an excess of HCO_3^- and CO_3^{2-}, generated by carbonate and silicate weathering, into the marine environment. Carbonate weathering is particularly important in the southern and southeastern catchment regions of the Baltic Sea, where soils rich in limestone and organic matter (OM) favor the dissolution of solid calcium carbonate. CO_2 generated in soils from OM mineralization enhances the dissolution of carbonate minerals by driving the protonation of CO_3^{2-} ions to form HCO_3^-, thereby decreasing the degree of calcium carbonate saturation and triggering further dissolution of carbonates. The net reaction for the formation of alkalinity consisting mainly of HCO_3^- is given by Eq. 2.21:

$$CaCO_3 + CO_2 + H_2O \Rightarrow Ca^{2+} + 2HCO_3^- \tag{2.21}$$

Carbonate weathering is less important in the Baltic's Scandinavian catchment area, where siliceous primary rocks dominate the geological structures. Although silicates are also subjected to weathering by CO_2 and generate carbonate alkalinity, this process is much slower (Liu et al. 2011) than carbonate weathering. The complex chemical processes associated with CO_2-induced silicate weathering can be expressed by the following net reaction (Eq. 2.22):

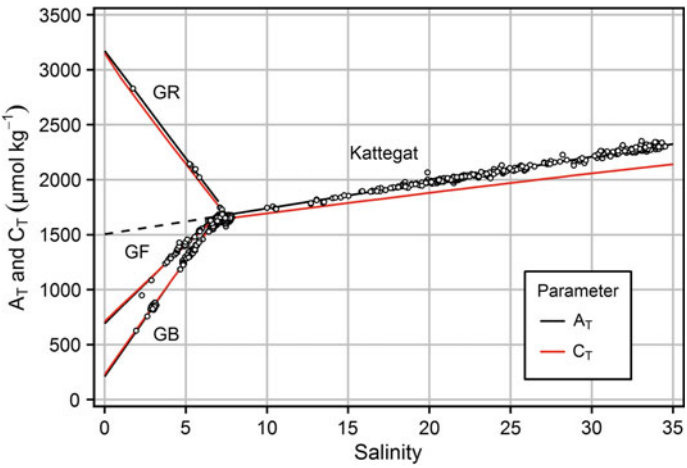

Fig. 2.6 Surface water alkalinity, A_T (*black*), and total CO_2, C_T (*red*), distributions as function of salinity in the Baltic Sea. The C_T levels are computed based on linear A_T-S-relations in the four sub-regions Kattegat, Gulf of Riga, Gulf of Finland and Gulf of Bothnia and assuming equilibrium with an atmospheric pCO_2 of 400 µatm and T = 10 °C (modified after Müller et al. 2016 with observations for the period 2008–2010)

$$CaSiO_3 + 2CO_2 + H_2O \Rightarrow Ca^{2+} + 2HCO_3^- + SiO_2 \tag{2.22}$$

The differences between the weathering processes in the Scandinavian and central European catchments are clearly indicated by the characteristics of the regional surface water salinity-alkalinity relationships (Fig. 2.6). The linear relationships in the three major Gulfs (Fig. 3.1) differ and extrapolating each one to zero salinity yields the flow-weighted mean A_T of river water entering the individual Gulfs. Due to the reduced weathering efficiency in the Scandinavian catchment, rivers entering the Gulf of Bothnia have the lowest A_T ($\sim$200 µmol kg^{-1}). An intermediate value is obtained for the Gulf of Finland ($\sim$700 µmol kg^{-1}), and a very high mean A_T ($\sim$3000 µmol kg^{-1}) for the Daugava River, which discharges into the Gulf of Riga. High A_T values were also directly observed in Odra and Vistula Rivers and can be attributed to intense carbonate weathering in central European catchments. The three regression lines intersect at a salinity of $\sim$7. This salinity is characteristic of large areas of the central Baltic Sea, which acts as a mixing chamber for water masses originating from the different gulfs, adjacent rivers, and inflowing North Sea water. Accordingly, also within the salinity interval ranging from 7 in the central Baltic Sea to $\sim$35 in the North Sea, a clear, linear, alkalinity-salinity relationship is obtained. Extrapolation of this line to a salinity of 0 yields an alkalinity of $\sim$1500 µmol kg^{-1}, which can be interpreted as the flow-weighted mean A_T of all rivers discharging into the Baltic Sea (Müller et al. 2016).

To explain the high A_T in continental European rivers by carbonate weathering requires a soil pCO_2 of several thousand µatm. Once the respective groundwater comes into contact with the atmosphere during its transport into the Baltic Sea, gas

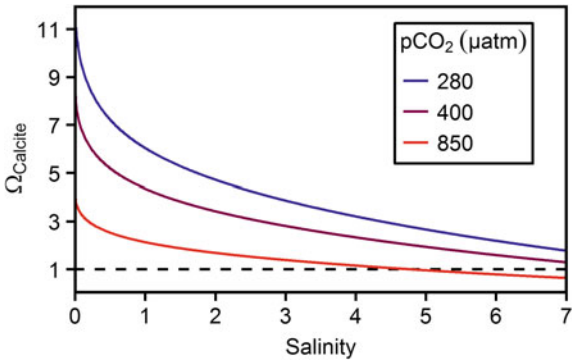

Fig. 2.7 Calcite saturation, $\Omega_{Calcite}$, as a function of salinity for the mixing of river water from the southern drainage basin (S = 0, A_T = 3000 µmol kg^{-1}) with Central Baltic Sea water (S = 7, A_T = 1650 µmol kg^{-1}). Calculations are performed for equilibrium with preindustrial (280 µatm), current (400 µatm) and worst case future (850 µatm) atmospheric pCO_2 levels and T = 5 °C

exchange occurs and the pCO_2 more or less adapts to the atmospheric pCO_2 level. During the release of CO_2, the CO_3^{2-} concentrations increase and the water becomes oversaturated with $CaCO_3$. Nonetheless, there is no precipitation of solid $CaCO_3$ because this process is inhibited, probably by the presence of magnesium ions (Berner 1975). However, the $CaCO_3$ oversaturation in river water decreases as the latter mixes with Baltic Sea water. This effect is illustrated in Fig. 2.7, which shows the degree of calcite saturation, $\Omega_{Calcite}$, as a function of salinity at a temperature of 5 °C for a river water A_T of 3000 µmol kg^{-1}. At the current atmospheric CO_2 content of ~400 ppm, the Ω for river water is ~8 but it decreases rapidly during the mixing of river water with Baltic Sea water and approaches 1, which implies equilibrium with solid calcite at a salinity of 7 in the central Baltic Sea.

The generation of alkalinity by weathering is intimately connected with an increase of the total CO_2 in groundwater because dissolved CO_3^{2-} ions are continually transformed to HCO_3^- by their reaction with CO_2 generated by the mineralization of soil OM. Hence, the dissolution of $CaCO_3$ and the subsequent formation of HCO_3^- continue until the groundwater has reached equilibrium with respect to both the dissociation of carbonic acid and the solubility of $CaCO_3$. The coupling of A_T and C_T at a given pCO_2 exists also in the Baltic Sea surface water, hence, at equilibrium with the atmospheric CO_2, A_T controls the C_T of seawater. As a result of this relationship, the plot of C_T versus S resembles that of A_T versus S (Fig. 2.6), although the relationship between A_T and C_T is not strictly linear.

2.3.4 Physico-Chemical Properties of the Master Variables

As total CO_2 (C_T) and total alkalinity (A_T) are conservative variables when related to mass units of seawater (e.g., µmol kg^{-1}) any changes in temperature or pressure

will cause only a shift in the relative contributions of the chemical species that represent them (Eqs. 2.15 and 2.18) without affecting their magnitude. This conservative behavior is also reflected in the mass conservation that occurs during the mixing of two water masses (m_1, m_2) with different C_T or A_T values (c_1, c_2), as shown in Eqs. 2.23 and 2.24:

$$m_1 \cdot c_1 + m_2 \cdot c_2 = (m_1 + m_2) \cdot c_{mix} \tag{2.23}$$

or

$$c_{mix} = \frac{m_1 \cdot c_1 + m_2 \cdot c_2}{m_1 + m_2} \tag{2.24}$$

Due to their conservative properties, C_T and A_T are key variables in model simulations (e.g. Omstedt et al. 2014; Gustafsson 2012; Kuznetsov et al. 2011), where they are subjected to mixing and biogeochemical transformations and thus control changes in pCO_2 and in the hydrogen ion concentration, $[H^+]$. The latter variables are derived from C_T and A_T by the use of the equilibrium constants K_0, K_1, and K_2 (Eqs. 2.4, 2.8 and 2.11). Hence, pCO_2 and $[H^+]$ (expressed as pH) depend on temperature and pressure (depth) and are thus called "non-conservative." The non-conservative properties of $[H^+]$ are also reflected in its behavior during the

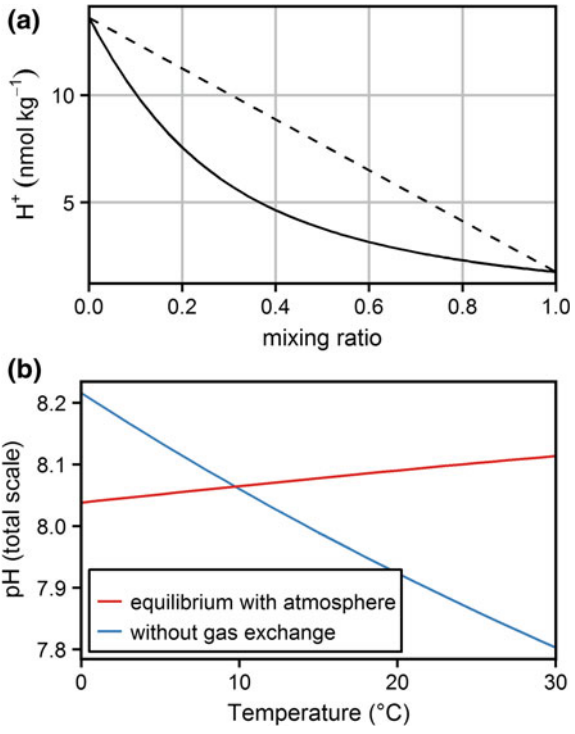

Fig. 2.8 Non-conservative behavior of the hydrogen ion concentration in seawater. **a** H^+ ion concentrations as a function of the mixing ratio of two water masses with different initial $[H^+]$, but the same A_T = 1670 µmol kg^{-1}, S = 7 and T = 10 °C (*solid line*). Hypothetical conservative mixing of $[H^+]$ is indicated by the *dashed line*. **b** Temperature dependency of pH during warming of the same water mass without gas exchange (C_T = const., 1640 µmol kg^{-1}) and in case that equilibrium with the ambient air is maintained (pCO_2 = const., 400 µatm)

mixing of different water masses. This is illustrated in Fig. 2.8a, which shows $[H^+]$ as a function of the mixing ratio of two water masses with the same temperature, salinity, and alkalinity, but different pH. The $[H^+]$ shows a distinct non-linear dependency on the mixing ratio and the differences with regard to a hypothetical conservative mixing line (Eq. 2.24) may be >30%.

The temperature dependency of non-conservative variables is especially important for the pCO_2 because along with biological activity it controls the seasonality of the surface water pCO_2, which in turn controls CO_2 gas exchange with the atmosphere. Furthermore, since in many cases pCO_2 cannot be measured at the in situ temperature, it is necessary to know the temperature coefficient to allow a correction. The temperature coefficient is commonly defined by the relative change of the pCO_2 per K, which is mathematically equivalent to $d(\ln pCO_2)/dT$. For oceanic systems, the experimentally derived coefficient of 0.0423 K^{-1} (Takahashi et al. 1993), corresponding to a 4.23% change in pCO_2 per unit K, is a reasonable approximation. However, the values may be significantly lower (as low as 3% K^{-1}) at concurring low salinities and alkalinities, as observed in the Gulf of Bothnia (see Box 2.3 for details).

Box 2.3: Temperature dependency of pCO_2

The relative change in pCO_2 induced by a change in temperature, $d(\ln pCO_2)/dT$, was experimentally determined as 0.0423 K^{-1} for largely stable and homogeneous oceanic conditions (Takahashi et al. 1993). This coefficient is used, for example, to estimate the reaction of pCO_2 upon the warming of ocean waters, or to correct the measured pCO_2 values to the in situ temperature. As for any other gas dissolved in water, the change in pCO_2 as a function of temperature is directly related to the change in the solubility constant K_0 (Eq. 2.14, Fig. 2.2). However, for CO_2 the temperature

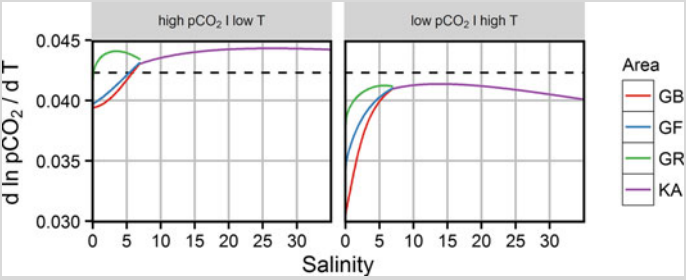

Fig. B3.1 The temperature (T) dependency of pCO_2 expressed as the relative change in pCO_2 per °K, $(d(\ln pCO_2)/dT)$. Values are given as a function of salinity for the different alkalinity and salinity regimes (compare with Fig. 2.6) encountered in the Gulf of Bothnia (GB), Finland (GF), and Riga (GR), as well as for the transition from the central Baltic Sea to the North Sea (the Kattegat, KA). The panels show typical winter (high pCO_2 = 500 µatm, low T = 5 °C) and summer (low pCO_2 = 300 µatm, high T = 20 °C) conditions. The dashed horizontal line indicates the experimentally derived value (0.0423 K^{-1}) for oceanic conditions

dependency of the partial pressure is also impacted by temperature-induced changes in the dissociation constants K_1 and K_2 that control the concentration of CO_2^*. Therefore, the coefficient depends on the compositions of the seawater, expressed by its salinity and alkalinity, and on the speciation of the CO_2 system components, controlled by the temperature and pCO_2. For the complex S, A_T, T, and pCO_2 conditions in the Baltic Sea, the coefficient d $(\ln pCO_2)/dT$ can differ significantly from 0.0423 K^{-1}. Figure B3.1 presents the coefficient as a function of the salinity, calculated for the typical seawater composition of sub-regions of the Baltic Sea and for a combination of T and pCO_2 that roughly reflects winter and summer conditions. The deviations of the coefficient from the empirical oceanic value of 0.0423 K^{-1} are largest in the areas approaching the inner gulfs, for example, 0.036 K^{-1} (−15%) at S = 2 in the Gulf of Bothnia during summer. However, the salinity of the bulk of Baltic Sea surface water investigated in this book is between 5 and 10 and the corresponding deviation from oceanic value is <5% and thus in most cases negligible.

Likewise, the temperature dependency of pH is also a function of alkalinity and is influenced by salinity. In the absence of gas exchange with the atmosphere (C_T = constant), the pH of seawater decreases during warming. This is illustrated by the blue line in Fig. 2.8b, which shows the pH as a function of temperature at an alkalinity of 1600 μmol kg^{-1} and a salinity of 7, conditions typical for the central Baltic Sea. The pH decrease amounts to ∼0.01 per K and corresponds to a relative increase in $[H^+]$ of ∼2.3% per K. If the equilibrium with ambient air is maintained (pCO_2 = constant) during warming by spontaneous gas exchange, the loss of CO_2 reverses the temperature dependency of the pH and results in a slight increase of the pH.

To estimate qualitatively the effect of any biogeochemically or physically induced change in the marine CO_2 system, it is useful to consider the combined dissociation equilibria for carbonic acid. Dividing the equilibrium equation for the first dissociation step (Eq. 2.8) by that for the second dissociation step (Eq. 2.11), yields the relationship shown in Eq. 2.25:

$$\frac{[HCO_3^-]^2}{[CO_2^*] \cdot [CO_3^{2-}]} = \frac{K_1}{K_2} \tag{2.25}$$

This equation refers formally to the reaction described by Eq. 2.26:

$$CO_2 + CO_3^{2-} + H_2O = 2HCO_3^- \tag{2.26}$$

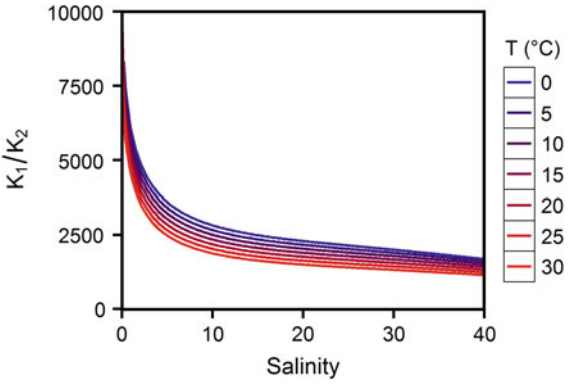

Fig. 2.9 Ratio of the dissociation constants K_1/K_2 as a function of salinity and temperature. The K_1/K_2 ratio formally corresponds to the equilibrium constant of the CO_2 buffer reaction (Eq. 2.25)

which is also known as "buffer reaction" in the context of the oceanic uptake of anthropogenic CO_2. The buffer equation does not account for the existence of hydrogen ions, which are involved in any reaction concerning the CO_2 system. However, the concentrations of H^+ are several orders of magnitude lower than those of the CO_2 species. Hence, any re-equilibration of the CO_2 system after the addition/removal of CO_2 or CO_3^{2-} occurs mainly by a shift in the relative distribution of the CO_2 species, which can be estimated from Eq. 2.25 or from the underlying reaction (Eq. 2.26). Thus, during the uptake of anthropogenic CO_2, most of the dissolved anthropogenic CO_2 is converted to HCO_3^- (buffered) by its reaction with CO_3^{2-}. Furthermore, the temperature and salinity dependency of K_1/K_2 allows an assessment of the corresponding changes in the relative distribution of the CO_2 species. Both increasing temperature and, in particular, increasing salinity lower the K_1/K_2 ratio (Fig. 2.9) and, according to Eqs. 2.25 and 2.26, increase the concentrations of CO_2^* and of CO_3^{2-} at constant C_T. The presence of the latter ions favors the formation of calcium carbonate shells and supports the high abundances of calcifying organisms, e.g., corals, in the high-temperature and high-salinity sub-tropic ocean.

The Revelle factor, which describes the relative change in pCO_2 in response to the relative change of total CO_2, is a further useful quantity to characterize the marine CO_2 system; it is defined in Eq. 2.27:

$$\frac{d(\ln pCO_2)}{d(\ln C_T)} = R \tag{2.27}$$

Assuming that the global ocean surface is, on average, approximately at equilibrium with the atmospheric CO_2, the Revelle factor can be used to assess the capacity of ocean surface water to take up anthropogenic CO_2, because R indicates how much CO_2 must be taken up by the water to achieve a new equilibrium with the atmospheric CO_2 after anthropogenic perturbation. Low R values imply that more anthropogenic CO_2 can be stored in the ocean at the expense of the fraction that stays in the atmosphere, and vice versa.

However, in many cases it is more informative to describe the relationship between C_T and pCO_2 by the differential quotient of their absolute values, R^* (Eq. 2.28):

$$\frac{dpCO_2}{dC_T} = R^* \tag{2.28}$$

In Chap. 5, changes in C_T are calculated from pCO_2 measurements to estimate net OM production. The sensitivity of this approach is represented by R^*, since it quantifies the signal in the measured pCO_2 that is triggered by the loss of C_T. R^* is related to the ratio $[CO_2^*]/[CO_3^{2-}]$ which in turn is a complex function of A_T, pCO_2, temperature, and salinity. The magnitude of the surface-water R^* is presented as a function of the pCO_2 in Fig. 2.10 for the main sub-regions of the Baltic Sea. The considered pCO_2 range of 100–600 µatm approximately reflects the seasonal pCO_2 variability encountered in the Baltic Proper and adjacent coastal areas, and

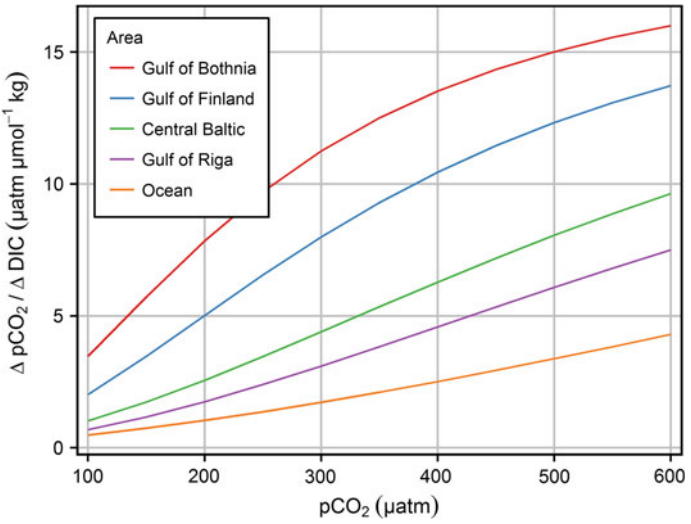

Fig. 2.10 Changes of pCO_2 upon changes in C_T ($R^* = \Delta pCO_2/\Delta C_T$) as a function of the pCO_2 level in different water masses: Gulf of Bothnia (S = 3, A_T = 800 µmol kg^{-1}), Gulf of Finland (S = 3, A_T = 1200 µmol kg^{-1}), Central Baltic (S = 7, A_T = 1670 µmol kg^{-1}), Gulf of Riga (S = 3, A_T = 2600 µmol kg^{-1}) and ocean water (S = 35, A_T = 2300 µmol kg^{-1}) at T = 10 °C. Highest R^* values result from low CO_3^{2-} concentrations, e.g., in water with low A_T and high pCO_2 levels

corresponds to an increase of R^* by a factor of 6–7. Similarly, alkalinity has a strong effect on R^*, leading to highest and lowest R^* values in the Gulf of Bothnia and ocean water, respectively. The regional and seasonal variability of R^* is thus considerable and has implications for the sensitivity and uncertainties associated with our approach to estimating changes in total CO_2 from pCO_2 measurements.

2.4 CO_2 Air-Sea Gas Exchange

In addition to its role in the characterization of the marine CO_2 system, pCO_2 is a major control of the CO_2 gas exchange between the sea surface and the atmosphere. The exchange at the sea surface of CO_2, O_2, N_2, or any other gas with a similarly low solubility is thermodynamically driven by the concentration gradient across the laminar layer at the air-sea interface. This layer, which is also referred to as the film layer or the viscous layer, is not influenced by turbulence and any transport of dissolved substances occurs by molecular diffusion. The thickness of the laminar layer depends on the physical state of the sea surface (wind speed) and is typically several tens of μm. Using a simple film model (Liss and Merlivat 1986), the flux, F, of any gas can be expressed as shown in Eqs. 2.29 and 2.30:

$$F = k \cdot (c^{sea} - c^{sat}) \tag{2.29}$$

or

$$F = k \cdot \Delta c \tag{2.30}$$

where c^{sea} is the concentrations of the gas in bulk seawater and represents the concentration at the lower boundary of the laminar layer, and c^{sat} is the saturation concentration of the gas presumed to be present at the upper boundary of the laminar layer. This interpretation of the flux equation is based on the assumption that the exchange of gases with low solubilities is entirely controlled by transfer across the laminar layer at the water surface (water-side control). By contrast, the exchange of gases with high solubilities, as is the case for many volatile organic substances and water vapor itself, is controlled by the concentration gradient in the gas phase. If the exchanged gas is CO_2, c^{sea} and c^{sat} refer to CO_2^*, which represents the gaseous fraction of the dissolved CO_2 species. However, since CO_2^* cannot be measured directly and is only accessible by measurements of pCO_2 (Eq. 2.14), it is convenient to express Eq. 2.30 as Eq. 2.31:

$$F = k \cdot K_o \cdot (p\mathrm{CO}_2 - p\mathrm{CO}_2^{atm}) \tag{2.31}$$

or

$$F = k \cdot K_o \cdot \Delta p\mathrm{CO}_2 \tag{2.32}$$

where ΔpCO_2 is the partial pressure difference between the surface water $pCO_2$and the atmospheric pCO_2. It is commonly used to characterize the CO_2 saturation of seawater with regard to atmospheric CO_2 although the fugacity difference (ΔfCO_2) is the correct thermodynamic representation.

The dynamic of the gas exchange is given by the transfer velocity k, which depends on the diffusion coefficient of the gas in seawater and on the thickness and stability of the laminar layer. The latter are influenced by microphysical processes, most of which are wind-controlled. Therefore, most of the existing bulk parameterizations of k are based on wind speed and many empirical equations have been suggested that describe k, at standard conditions of 20 °C and a salinity of 35, as a function of the wind speed, u (Wanninkhof 1992). The conversion of k to any other temperature and salinity requires the Schmidt number, Sc (Wanninkhof 1992), which is defined as the ratio between the kinematic viscosity and the diffusion coefficient. Although both are a function of temperature and salinity, variations of Sc for seawater are predominantly caused by temperature, because of the pronounced temperature dependency of the diffusion coefficient. By contrast, the effect of salinity on Sc is low and can generally be ignored. A reciprocal proportionality between the square root of Sc and k is assumed. Since the value of Sc at 20 °C and a salinity of 35 is 660, the transfer velocity k at any Sc calculated from the respective temperature and salinity is given by Eq. 2.33:

$$k = k_{660}(u) \cdot \left(\frac{660}{Sc(T,S)}\right)^{0.5} \tag{2.33}$$

The exponent 0.5 is not a physical constant but a widely used experimental approximation. For the CO_2 flux calculations in the following sections we use the quadratic equation for k_{660}(u) shown in Eq. 2.34 and suggested by Wanninkhof et al. (2009):

$$k_{660} = 0.24u^2 \tag{2.34}$$

The coefficient of 0.24 applies to wind speed in m s^{-1} and yields k_{660} in cm h^{-1}.

Equations 2.31–2.34 are used to determine the CO_2 flux for a given partial pressure difference and to estimate the balance of the air-sea CO_2 gas exchange on the basis of pCO_2 time series data. It is based on the film model that accounts for the molecular diffusion of CO_2 through the laminar layer. However, a gradient of CO_2 across the laminar layer also implies gradients for HCO_3^- and CO_3^{2-} if equilibria within the CO_2 system are established. Thus, an additional net C_T flux occurs by the diffusion of HCO_3^- and CO_3^{2-} that can be accounted for by introducing a chemical enhancement factor into Eq. 2.33. However, the establishment of the CO_2 hydration equilibrium (Eq. 2.2) at the interface between the film layer and the atmosphere is relatively slow and at higher wind speeds lags behind the continuous renewal of the surface layer by turbulence. This hampers the formation of additional HCO_3^- and CO_3^{2-} gradients across the film layer such that a significant increase (>10%) of the air-sea CO_2 flux by chemical enhancement can only be expected at wind speeds

<4 m s^{-1} (Kuss and Schneider 2004). However, these estimates are associated with considerable uncertainty; thus, chemical enhancement of the CO_2 gas exchange is usually neglected in view of other uncertainties in the CO_2 flux calculations that are mainly due to the determination of k_{660}.

A further important characteristic of the air-sea gas exchange of any dissolved gas is the equilibration time, which characterizes the decrease in the concentration difference (Eq. 2.29) or the partial pressure difference (Eq. 2.32) across the film layer during gas exchange until a final equilibration with the ambient air is reached. This requires integration over time of the flux equation (Eq. 2.29), which can easily be performed for gases such as O_2 or N_2 that do not react with water (Box 2.4). Assuming that the atmospheric concentration of the considered gas is not affected by the gas exchange (c^{sat} = constant, see Eq. 2.29), the integration from t = 0 to any time t yields Eq. 2.35:

$$\Delta c(t) = \Delta c(t=0) \cdot \exp -\frac{k}{z_{mix}} \cdot t \tag{2.35}$$

where z_{mix} represents the depth of the mixed layer within which the gas gain or loss caused by gas exchange is homogenously distributed. According to the film model, the gas concentration in the mixed layer corresponds to the concentration at the lower boundary of the laminar layer.

According to Eq. 2.35, a perfect equilibrium between the water and the atmosphere ($\Delta c = 0$) is only achieved after an infinite time. This is a consequence of the mathematical idealization of the involved processes. To nonetheless quantify the dynamic of the equilibration process, the ratio z_{mix}/k, which has the unit "time," is used to characterize the equilibration process and is called the equilibration time (τ), described in Eqs. 2.36 and 2.37:

$$\tau = \frac{z_{mix}}{k} \tag{2.36}$$

$$\Delta c(t) = \Delta c(t=0) \cdot \exp -t/\tau \tag{2.37}$$

Hence, if the elapsed time after the start of the equilibration process is equal to τ, then $\Delta c(t)/\Delta c(t = 0)$ is equal to $e^{-1} = 0.36$. In other words, τ is the time after which 36% of the original $\Delta ct = 0$ still exists or, conversely, 64% of the original disequilibrium is compensated by gas exchange. Therefore, τ is also called the e-fold equilibration time. For O_2 gas exchange at a mean wind speed of 7 m s^{-1}, a mixed-layer depth of 30 m, and a temperature of 10 °C, τ is equal to 7 days.

Box 2.4: Integration of the flux equation

Here we consider the air-sea exchange of a gas that does not react with water (O_2, N_2, etc.). The basic equation used to calculate the flux (Eq. 2.29) is:

$$F = k \cdot (c^{sea} - c^{sat}) \tag{B4.1}$$

where the flux, F, is defined by the number of moles, dn, that pass the air-sea interface per time, dt, and area, A:

$$F = \frac{dn}{dt \cdot A} \tag{B4.2}$$

Hence, B4.1 can be written as:

$$\frac{dn}{dt \cdot A} = k \cdot (c^{sea} - c^{sat}) \tag{B4.3}$$

dividing by the depth of the mixed layer, z_{mix}, gives:

$$\frac{dn}{dt \cdot A \cdot z_{mix}} = k/z_{mix} \cdot (c^{sea} - c^{sat}) \tag{B4.4}$$

where $A \times z_{mix}$ represents the water volume that is affected by the addition/removal of dn moles of the gas. Hence, the gas exchange can be expressed in terms of the concentration changes in bulk seawater, dc^{sea}:

$$-\frac{dc^{sea}}{dt} = k/z_{mix} \cdot (c^{sea} - c^{sat}) \tag{B4.5}$$

According to the definition of Δc (Eq. 2.29), the flux will have a positive sign if it is directed from the water into the atmosphere. Hence, the change in the concentration in the water, dc^{sea}/dt, will have a negative sign. For the integration of Eq. 2.30, it is assumed that no other processes other than gas exchange affect Δc and that the change in the atmospheric concentration caused by the gas flux is negligible (c^{sat} = constant). The latter assumption implies that dc = d(Δc):

$$-\frac{d(\Delta c)}{dt} = k/z_{mix} \cdot \Delta c \tag{B4.6}$$

which can also be expressed as:

$$d(\ln \Delta c) = -k/z_{mix} \cdot dt \tag{B4.7}$$

The integration of which yields:

$$\ln \frac{\Delta c(t)}{\Delta c(t=0)} = -k/z_{mix} \cdot t \tag{B4.8}$$

or

$$\Delta c(t) = \Delta c(t=0) \cdot \exp -k/z_{mix} \cdot t \tag{B4.9}$$

The description of the equilibration process by gas exchange is more complicated for CO_2. The flux calculations are based on the diffusion of CO_2^*, but changes in the concentrations must refer to C_T since the CO_2^* flux affects the concentrations of all CO_2 species according to the CO_2 dissociation equilibria (Eqs. 2.8, 2.11, 2.26). To maintain the equilibrium between the CO_2 species in water, the major fraction of the CO_2 added by gas exchange in case of undersaturation must react with CO_3^{2-} to form HCO_3^-. Conversely, in case of CO_2 oversaturation, the major fraction of the CO_2 removed from the water is replaced by the conversion of HCO_3^- to CO_2 and CO_3^{2-} (Eq. 2.26). Therefore, only a certain fraction of the exchanged CO_2* contributes to the reduction of the disequilibrium that is reflected in the CO_2^* gradient across the laminar surface layer. This means that c^{sea} in the flux equation (Eq. 2.29) refers to CO_2^*, whereas the concentration change caused by the flux F must be described in terms of total CO_2, C_T, as described in Eqs. 2.38–2.41:

$$F = k \cdot ([CO_2^{*,sea}] - [CO_2^{*,sat}]) \tag{2.38}$$

or (see Box 2.4):

$$\frac{dC_T}{dt} = k/z_{mix} \cdot ([CO_2^{*,sea}] - [CO_2^{*,sat}]) \tag{2.39}$$

introducing the variable, f_D (dimensionless delay factor):

$$f_D = \frac{d[CO_2^{*,sea}]}{dC_T} \tag{2.40}$$

yields:

$$\frac{d[CO_2^{*,sea}]}{dt} = f_D \cdot k/z_{mix} \cdot ([CO_2^{*,sea}] - [CO_2^{*,sat}]) \tag{2.41}$$

The variable f_D is, by definition, equal to 1 for non-reactive gases and <1 in case of CO_2 dissolved in seawater. We will refer to it as the delay factor in the equilibration of the marine CO_2 system with atmospheric CO_2 since it reduces the term k/z_{mix}, previously defined as the reciprocal equilibration time for non-reactive gases. However, f_D is not a constant but rather a complex function of the state of the CO_2 system. As such, it changes during the equilibration process. This implies that there is no strict exponential decay of ΔpCO_2 during equilibration, nor exists a well-defined equilibration time as for non-reactive gases.

However, to illustrate the equilibration of the CO_2 system, the gas-exchange process has been numerically simulated based on Eq. 2.41 (Box 2.4). The

calculations derive from the same scenario used to determine the equilibration time for O_2 (wind speed = 7 m s^{-1}, z_{mix} = 30 m, sea surface temperature = 10 °C, S = 7). Assuming an initial air-sea disequilibrium, ΔpCO_2, the temporal development of the equilibration process by CO_2 gas exchange was calculated for finite time intervals. Since the dynamics of the equilibration depend on the delay factor (Eqs. 2.40 and 2.41) and thus on the state of the marine CO_2 system, separate calculations were performed for the five different water masses with characteristic alkalinity and salinity regimes: the Gulfs of Bothnia, Finland and Riga, the central Baltic Sea, and ocean water. The curves in Fig. 2.11 show the decrease in ΔpCO_2 over time, expressed as a percentage of the initial value. The equilibration curve for O_2 (Eq. 2.35), which must be the same for the different regions, is also included in the figure. After passage of the e-fold equilibration time τ, 63% of the original disequilibrium is compensated by gas exchange (horizontal line). For the selected conditions and in the case of oxygen, τ is roughly equal to 7 days. Although CO_2 does not have a defined e-fold equilibration time, the 63% equilibrium level is also used for it. In all cases τ is much larger for CO_2 than for O_2, with differences varying by factors between 3 (Gulf of Bothnia) and 10 (ocean water). This implies that any changes in the CO_2 system due to OM production or mineralization are conserved for a longer time in surface water than is the corresponding O_2 signal. This finding underlines the advantage of using CO_2 instead of O_2 measurements for biogeochemical studies.

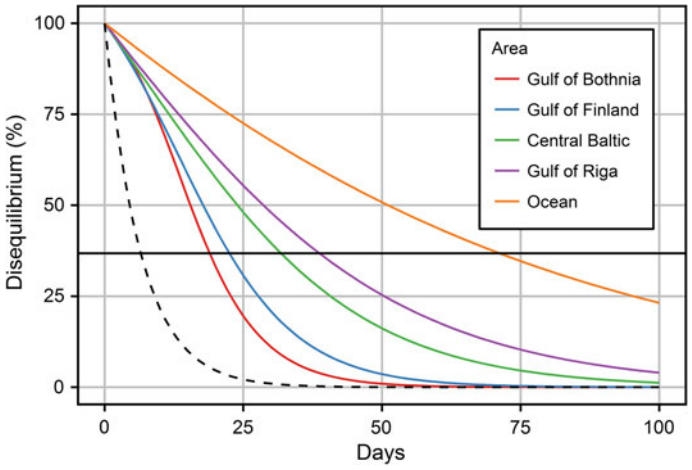

Fig. 2.11 Equilibration of O_2 (*black dashed line*) and of CO_2 (*colored lines*) with atmospheric O_2 and current CO_2. The equilibration of O_2 is characterized by an e-fold equilibration time after which 67% of the original horizontal disequilibrium is compensated for by gas exchange (*black horizontal line*). The equilibration of CO_2 is delayed and depends at a given pCO_2 mainly on the alkalinity. For the calculations we used the following parameters: Gulf of Bothnia (S = 3, A_T = 800 µmol kg^{-1}), Gulf of Finland (S = 3, A_T = 1200 µmol kg^{-1}), Central Baltic (S = 7, A_T = 1670 µmol kg^{-1}), Gulf of Riga (S = 3, A_T = 2600 µmol kg^{-1}) and ocean water (S = 35, A_T = 2300 µmol kg^{-1}) at T = 10 °C. The initial pCO_2 disequilibrium was in all sub-regions equivalent to a C_T drawdown of 50 µmol kg^{-1} from equilibrium with atmospheric pCO_2

In addition, the differences between the τ values for CO_2 in the different water masses are remarkable. Under the conditions defined in Fig. 2.11, the τ of ocean water is more than three times higher than that of water in the Gulf of Bothnia. This is due to the dependency of the delay factor f_D (Eq. 2.40) on the carbonate ion concentration, which is low in the Gulf of Bothnia because of the low alkalinity. Furthermore, the salinity affects the carbonate ion concentration (Fig. 2.9) because of greater dissociation at high salinities. Accordingly, τ is highest for ocean water although the highest alkalinity occurs in the Gulf of Riga. It must be noted that the equilibration curves in Fig. 2.11 demonstrate only the relative differences in τ for O_2 and CO_2 in water masses with differing alkalinity and salinity. To assess absolute τ values requires that other variables, such as the mixed-layer depth and wind speed (Eqs. 2.36 and 2.34), are taken into account. It must also be noted that the equilibration time is a theoretical quantity because under natural conditions disequilibria are incessantly generated by changing temperatures and biogeochemical processes. Nevertheless, it is a very useful quantity for understanding the response of the marine CO_2 system to the biogeochemical consumption or release of CO_2.

References

Berner RA (1975) The role of magnesium in the crystal growth of calcite and aragonite from sea water. Geochim Cosmochim Acta 39(4):489–504

Dickson AG (1984) pH scales and proton-transfer reactions in saline media such as sea water. Geochim Cosmochim Acta 48(11):2299–2308

Dickson AG (1981) An exact definition of total alkalinity and a procedure for the estimation of alkalinity and total inorganic carbon from titration data. Deep Sea Research Part A. Oceanographic Research Papers 28(6):609–623

Gustafsson E (2012) Modelling long-term development of hypoxic area and nutrient pools in the Baltic Proper. J Mar Syst 94:120–134

Kulinski K, Schneider B, Hammer K, Machulik U, Schulz-Bull D (2014) The influence of dissolved organic matter on the acid-base system of the Baltic Sea. J Mar Syst 132:106–115

Kuss J, Schneider B (2004) Chemical enhancement of the CO_2 gas exchange at a smooth seawater surface. Marine Chemistry, 91(1–4):165–174

Kuznetsov I, Neumann T, Schneider B, Yakushevm E (2011) Processes regulating pCO_2 in the surface waters of the central eastern Gotland Sea: a model study. Oceanologia 53:745–770

Lavigne H, Epitalon JM, Gattuso J-P (2011) Seacarb: seawater carbonate chemistry with R. http://cran.r-project.org/package=seacarb

Le Quéré C, Andrew RM, Canadell JG et al (2016) Global Carbon Budget 2016. Earth Syst Sci Data 8:605–649

Liss PS, Merlivat L (1986) Air-sea gas exchange: introduction and synthesis. In: Buat-Menard P (ed) The role of air-sea exchange in geochemical cycling. NATO ASI series, C 185, Reidel, pp 113–127

Liu Z, Dreybrodt W, Liu H (2011) Atmospheric CO_2 sink: silicate weathering or carbonate weathering? Appl Geochem 26(Supplement):S292–S294

Millero FJ, Graham TB, Huang F, Bustos-Serrano H, Pierrot D (2006) Dissociation constants of carbonic acid in seawater as a function of salinity and temperature. Marine Chemistry 100(1–2):80–94

Millero FJ (2010) Carbonate constants for estuarine waters. Mar Freshwater Res. 61:139–142
Milliman JD (1975) Dissolution of aragonite, Mg-calcite, and calcite in the North Atlantic Ocean. Geology 3:461–462. doi:10.1130/0091-7613(1975)
Müller JD, Schneider B, Rehder G (2016) Long-term alkalinity trends in the Baltic Sea and their implications for CO_2-induced acidification. Limnol Oceanogr 61:1984–2002. doi:10.1002/lno.10349 –open access–
Omstedt A, Humborg C, Pempkowiak J, Perttilä M, Rutgersson A, Schneider B, Smith B (2014) Biogeochemical control of the coupled CO_2–O_2 system of the Baltic Sea: a review of the results of Baltic-C. Ambio 43(1):49–59
Pierrot D, Lewis DE, Wallace DWR (2006) MS Excel program developed for CO_2 system calculations. ORNL/CDIAC-105a. Carbon Dioxide Information Analysis Center, Oak Ridge National Laboratory, U.S. Department of Energy, Oak Ridge, Tennessee. doi:10.3334/CDIAC/otg.CO2SYS_XLS_CDIAC105a
Schneider B, Gülzow W, Sadkowiak B, Rehder G (2014) High potential of VOS-based measurements in Baltic Sea surface waters for detecting sinks and sources of carbon dioxide and methane. J Mar Syst 140:13–25
Soli AL, Byrne RH (2002) CO_2 system hydration and dehydration kinetics and the equilibrium CO_2/H_2CO_3 ratio in aqueous NaCl solution. Mar Chem 78:65–73
Takahashi T, Olafsson J, Goddard JG, Chipman DW, Sutherland SC (1993) Seasonal variation of CO_2 and nutrient salts in the high latitude oceans: a comparative study. Glob Biogeochem Cycles 7:843–848
Tyrrell T, Schneider B, Charalampopoulou A, Riebesell U (2008) Coccolithophores and calcite saturation state in the Baltic and Black Seas. Biogeosciences 5:1–10
Wanninkhof R (1992) Relationship between wind speed and gas exchange over the ocean. J Geophys Res 97:7373–7382
Wanninkhof R, Asher WE, Ho DT, Sweeney C, McGillis WR (2009) Advances in quantifying air-sea gas exchange and environmental forcing. Annu Rev Mar Sci 1(1):213–244
Weiss RF (1974) Carbon dioxide in water and seawater: the solubility of a non-ideal gas. Mar Chem 2:203–215

http://www.springer.com/978-3-319-61698-8

Biogeochemical Transformations in the Baltic Sea
Observations Through Carbon Dioxide Glasses
Schneider, B.; Müller, J.D.
2018, XII, 110 p. 54 illus., Hardcover
ISBN: 978-3-319-61698-8